Single-Step Preparation of TiO₂/MWCNT Nanohybrid Materials by Laser Pyrolysis and Application to Efficient Photovoltaic Energy Conversion

Jin Wang,[†] Yaochen Lin,[†] Mathieu Pinault,[†] Arianna Filoramo,[‡] Marc Fabert,[§] Bernard Ratier,[§] Johann Bouclé,*[,§] and Nathalie Herlin-Boime*[,†]
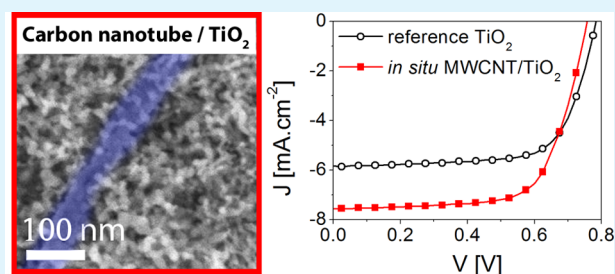
[†]IRAMIS/NIMBE/LEDNA LFP, CEA-CNRS URA 2453, CEA de Saclay, 91191 Gif sur Yvette, France
[‡]DSM/IRAMIS/NIMBE/LICSEN, CEA de Saclay, 91191 Gif sur Yvette, France
[§]XLIM UMR 7252, Université de Limoges/CNRS, 87060 Limoges Cedex, France

Ⓢ *Supporting Information*

ABSTRACT: This paper presents the continuous-flow and single-step synthesis of a TiO₂/MWCNT (multiwall carbon nanotubes) nanohybrid material. The synthesis method allows achieving high coverage and intimate interface between the TiO₂ particles and MWCNTs, together with a highly homogeneous distribution of nanotubes within the oxide. Such materials used as active layer in the porous photoelectrode of solid-state dye-sensitized solar cells leads to a substantial performance improvement (20%) as compared to reference devices.

Implementing carbon nanotubes (CNTs) into dye-sensitized solar cells (DSSCs) is a promising strategy to improve charge collection efficiency.[1,2] Because of their excellent electrical properties, CNTs can indeed improve both charge separation and electron transport in the optoelectronic devices. They were thereby applied or incorporated in all components of DSSCs, including counter electrodes[3] and electrolyte.[4] Concerning the dye-sensitized porous TiO₂ working electrode (WE), different types of CNTs (multiwall[2,5,6] or single wall,[1] bare[5] or functionalized[2,6]) were also added to reduce charge recombination and to improve charge collection. An optimal CNTs concentration in TiO₂ was found in the range 0.01[7] to 0.3 wt %,[2] leading to performance improvements on the order of 18−26% with regard to reference devices based on pure TiO₂ mesoporous anode.[5,8] However, all these studies were carried out on liquid or quasi-solid DSSCs, and no studies have been published on solid-state cells, despite the strong potentialities that have been recently demonstrated for both dye-sensitized[9] or perovskite-sensitized devices.[10]

Such nanocomposite materials can be obtained through varieties of methods: many studies now report mechanical mixing of TiO₂ pastes with CNTs in solution,[7] or growth of TiO₂ at the surface of CNT by sol gel chemistry.[6] Some advanced methods are also reported such as the use of virus-templated self-assembly,[1] electrospinning,[5] controlled phase separation,[11] modified sol−gel methods,[12] modified ultrasonication method,[13] chemical vapor deposition,[14] or hydrothermal synthesis.[15] In most cases, the CNT surfaces are modified to achieve better TiO₂/CNTs electronic contacts and

obtain the targeted beneficial effects. The preparation methods that affect the CNT surface are for example chemical oxidation treatment[11,16] or plasma-modified methods.[2] Most of these methods are "non-continuous" and remain unadapted for industrial applications. By contrast, the laser pyrolysis used here is a gas phase method producing nanoparticles in a flow and has already been developed at the scale of pilot plant.[17,18] It already demonstrated its versatility for the synthesis of various oxide and nonoxide nanoparticles[17] and proved to be a relevant technique for the production of low-cost TiO₂ nanoparticles well-suited for the photovoltaic applications.[19] The efficient single-step synthesis of TiO₂−CNT composites described here is a new example of this versatility.

The laser pyrolysis and the aerosol-assisted catalytic chemical vapor deposition (CCVD) methods have already been described for the synthesis of TiO₂ nanopowders[20,21] and MWCNT[22] respectively. Briefly (more details are provided in the Supporting Information), the laser pyrolysis is a flow method based on the resonance between the emission of a CO₂ laser at 10.6 μm and the absorption of a chemical precursor. In the case of TiO₂ nanoparticles, crystallinity is controlled by an adequate choice of laser power.[21] Droplets of precursor (titanium tetraisopropoxide, TTIP) are carried to the reaction zone together with an ethylen flow, ensuring laser absorption and efficient production of nanoparticles collected downstream

on metallic filters. Concerning the nanotubes, MWCNT were synthesized as aligned carpets in a quartz reactor from a precursor mixture of toluene in the presence of ferrocene, used as catalytic agent. For this study and after a conventional annealing step (removal of the residual catalyst), the MWCNT were dispersed by high power ultrasonic probe in water containing a dispersing agent. They were also oxidized in a mixed solution of concentrated acids, filtered, and washed several times before use. Figures S1 and S2 in the Supporting Information show the efficiency of the oxidation treatment by detection of added oxygen content and CO bonding.

These nanotubes were then redispersed in toluene and mixed with TTIP for the synthesis by laser pyrolysis in a single step of in situ TiO_2/MWCNT composites (referred as MWCNT/TiO_2[in situ]). In this case, the TiO_2 particle growth is directly occurring "on-flight" at the MWCNT surface. A reference TiO_2 powder was obtained from a mixture of TTIP with the same amount of toluene. Finally, direct mixtures of MWCNT with the reference TiO_2 powder were also prepared to achieve ex situ composites (referred as MWCT/TiO_2[ex situ]) presenting various MWCNT contents from 0.01 to 0.3 wt %. Besides, the MWCNT content in the in situ composite was fixed to 0.03 wt % in this study, as this content was found to be quite optimal regarding the photovoltaic response in terms of device efficiencies for the ex situ devices (as reported in the Supporting Information, and in the following discussion). Therefore, this weight ratio was chosen for all characterizations presented in this manuscript, except for the ex situ sample where a higher content was used (0.1 wt %) to reach the detection limit of some characterization techniques. Applying this method, we are able to discuss the properties of our in situ sample with regard to the pure TiO_2 reference, in order to evaluate the relevance of CNT incorporation, and with regard to the ex situ sample of similar CNT content, in order to illustrate the relevance of laser pyrolysis for the application. Data corresponding to different CNT contents for the in situ composites are however given in the Supporting Information.

Figure 1a, b presents the transmission electron microscopy (TEM) images of the in situ and ex situ synthesized composites.

When the composite is formed in situ, the MWCNTs are covered with a high density of TiO_2 nanoparticles, leaving almost no bare nanotube surface. In the ex situ case where MWCNTs are mechanically mixed with TiO_2 particles already synthesized, only a partial coverage of the MWCNTs by TiO_2 nanoparticles is observed. These observations suggest that a stronger chemical grafting occurs at the MWCNT/TiO_2 interface using the in situ process, this particular morphology remaining unchanged after 30 min of high power sonication indicating efficient bonding between TiO_2 and MWCNT. Figure S3 in the Supporting Information gives the TEM length dispersion of the MWCNT, while the mean diameter of TiO_2 was obtained from Figure S4 in the Supporting Information and found to be 11.7 and 11.8 nm for the reference TiO_2 powder and in situ composite respectively (standard deviation 2.0, counting 100 nanoparticles). The specific surface areas of the powder samples are found to be around 122, 116, and 120 m^2/g for TiO_2, MWCNT/TiO_2[in situ] and MWCNT/TiO_2[ex situ] (0.03 wt % CNT) respectively. The corresponding diameter estimations (B.E.T. method) are around 12 nm (see Table S1 in the Supporting Information), in good agreement with TEM measurements and indicating that the low amount of MWCNT does not significantly contribute to
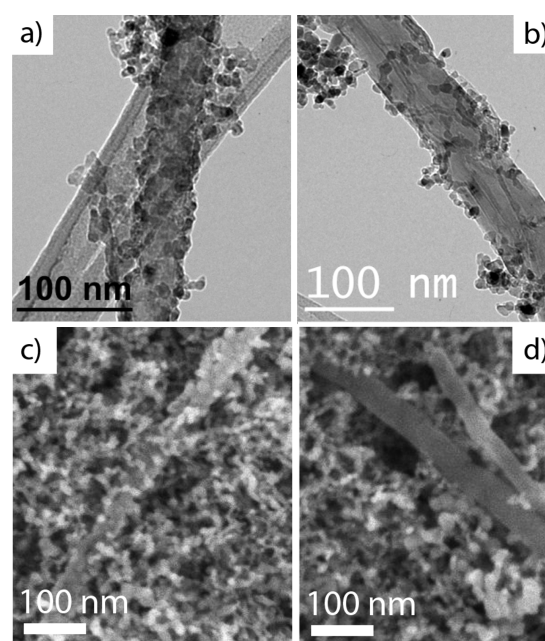

Figure 1. TEM images of (a) in situ and (b) ex situ MWCNTs/TiO_2 nanocomposites. SEM top view images of TiO_2 porous layers processed from (c) in situ and (d) ex situ composites.

the specific surface. The synthesized TiO_2 and MWCNT/TiO_2[in situ] powders contain more than 85% of anatase crystal phase (the TiO_2 crystallite mean diameter is around 10 nm). As expected, the crystallite size appears slightly smaller than the grain size evaluated from TEM ad BET. The XRD patterns are shown in the Supporting Information as Figure S5.

Considering that TEM gives only a very local representation of the sample, Raman spectroscopy was used to assess the presence of MWCNTs among the TiO_2 particles and their dispersion in the powder. A typical MWCNT/TiO_2 Raman spectrum shows both contributions arising from the TiO_2 anatase crystal structure and the pure MWCNT (see Figure S6 in the Supporting Information). In particular, two main bands are associated with the nanotubes at approximately 1330 and 1575 cm^{-1}, which can be assigned to the D (disorder mode) and G (tangential mode) bands of the MWCNTs, respectively.[5,16] Considering the separation of the TiO_2 and nanotubes active Raman modes, Raman mapping was performed on the TiO_2, MWCNT/TiO_2[in situ] and MWCNT/TiO_2[ex situ] powder samples by monitoring the intensity of the D-band over 40 × 40 square micrometers surfaces. For almost all cases, no signal associated with carbon phases could be detected from the pure TiO_2 sample, nor the ex situ sample using only 0.03 wt % of nanotube content. Only some random analysis gave some nanotube signatures due to the inherent inhomogeneity of the mixing between the synthesized TiO_2 powder and the nanotube sample (see Figure S7). The analysis was thus made on the MWCNT/TiO_2[ex situ] using 0.1 wt % of MWCNT. Figure 2a, b presents the corresponding Raman maps, as well as the 8-bit pixel distributions (Figure 2c), including that of pure TiO_2 (the Raman maps associated with the pure TiO_2 sample is given in the Supporting Information as Figure S7).

A very low color level is uniformly observed for the ex situ composite, indicating that only few carbon phases can be found over the analyzed region. By comparing different regions randomly selected on the sample, it is, however, possible to
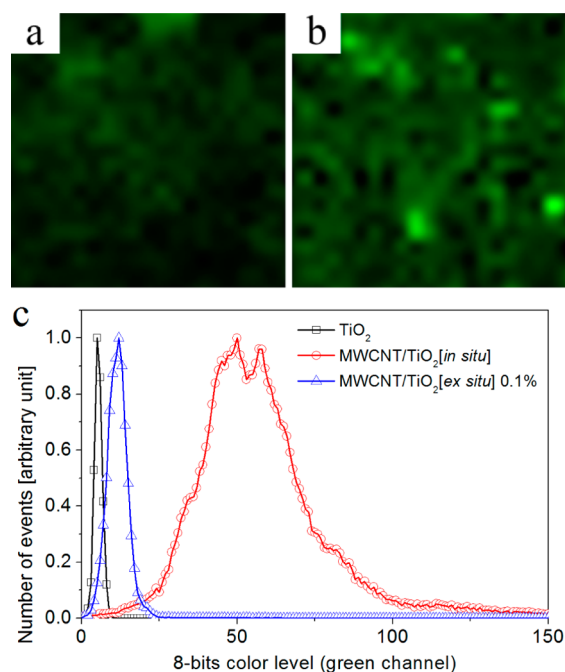
Figure 2. Raman maps over 40 × 40 square micrometers associated with the disorder mode (D band) of MWCNTs within (a) MWCNT/TiO₂[ex situ] and (b) MWCNT/TiO₂[in situ] composites, and (c) corresponding 8-bit pixel distributions where pure TiO₂ is also presented as reference. The CNT content is 0.03 and 0.1 wt % for the in situ and ex situ composites, respectively.

Figure 3. Photoluminescence (PL) spectra of TiO₂, MWCNT/TiO₂[ex situ], and MWCNT/TiO₂[in situ] (CNT contents of 0.03 wt % in each case).

observe highly intense regions (see Figure S6 in the Supporting Information), indicating that the MWCNT dispersion remains inhomogeneous in the sample elaborated from a direct postmixing. At the opposite, a highly homogeneous carbon signature is evidenced for the sample processed in situ. Furthermore, compared to the Raman spectrum of acid-treated MWCNT alone (see Figure S6 in the Supporting Information), the G band associated with MWCNTs exhibits a slight shift, which usually results from strain effects at the TiO₂/MWCNTs interfaces.[16] This shift is found to be larger in the case of the MWCNT/TiO₂[in situ] sample, suggesting better local interactions in this sample compared to the mixed ex situ sample, which is consistent with a better grafting of the TiO₂ particles at the CNT surface.

Photoluminescence (PL) spectroscopy is widely used to investigate the electron−hole fate in semiconductor particles[23,24] and is therefore highly relevant to monitor the electronic interactions between MWCNTs and semiconducting nanocrystals. Figure 3 shows the PL spectra of samples TiO₂, MWCNT/TiO₂[ex situ], and MWCNT/TiO₂[in situ] (MWCNT content of 0.03 wt % in each case, excitation at 300 nm). All spectra are normalized with regard to the free exciton emission peak of anatase at 3.15 eV (see the Supporting Information for experimental details and complementary photoluminescence spectra, Figure S8), allowing a direct comparison of the absolute intensities.

PL contributions below the optical band gap are generally associated with electron−hole recombination mechanisms occurring in the presence of electronic defects.[25,26] In our case, a clear contribution at 2 eV is visible for pure TiO₂ as well as for MWCNT/TiO₂ composites. This feature can be attributed to interfacial self-trapped electrons[24,27] which are thus found to be dependent on the local environment of the
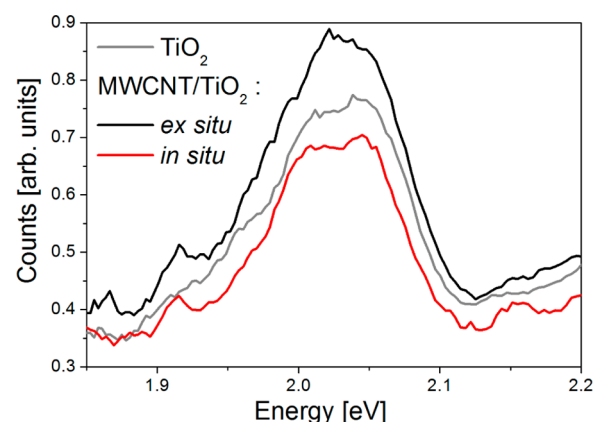
particles. We observe a slight but significant decrease in this feature for sample MWCNT/TiO₂[in situ] compared to pure TiO₂ and the ex situ sample. This observation is consistent with reduced radiative recombination of photoinduced electrons trapped at the TiO₂ particle surface. This indicates that efficient charge transfers to the nanotubes can occur.[24,28] It is worth noting that this PL decrease is found to be even much more pronounced for in situ samples containing 0.09 wt % CNT (see Figure S9 in the Supporting Information). Such observations suggest that our in situ process is highly favorable to achieve efficient electronic interactions between the two components compared to a postmixing process. These analyses show that the synthesized MWCNT/TiO₂[in situ] nanocomposites exhibit improved physical properties, highly suitable for the fabrication of efficient porous photoanodes to be used within dye-sensitized solar cells.

We thus finally compare our materials with regard to the photovoltaic application. To do so, porous photoelectrodes are prepared from the three nanopowders, following conventional paste formulation steps that have been previously developed (see ref 19 and the Supporting Information) to achieve 2 μm thick porous films on fluorinated tin oxide substrates. Benchmark materials (organic indoline D102 dye, spiro-OMeTAD hole transporter) were used as they allow a direct comparison of the porous electrodes. Device performance are assessed under simulated sunlight, including spectral mismatch correction, leading to an AM1.5G equivalent power density of 100 mW cm⁻² on the cells. Table S2 (see the Supporting Information) reports the photovoltaic performance of cells based on the ex situ composites for different CNT contents. From this set of devices, we fixed the CNT content to 0.03% for all composites as it is associated with the highest photovoltaic response, in accordance with the literature,[7] and prepare new independent sets of devices to achieve consistent comparisons for the composites. We thus present below the photovoltaic performance of a representative batch of ssDSSC based on the pure TiO₂ electrode, as well as our ex situ and in situ composites.

Figure 4a presents the current density−voltage characteristics of the cells. The photovoltaic parameters (photocurrent density J_{SC}, open-circuit voltage V_{OC}, fill factor FF, and power conversion efficiency η) are summarized in Table 1. Figure 4b shows the spectral response, or incident photon to charge carrier conversion efficiency (IPCE) of the devices.
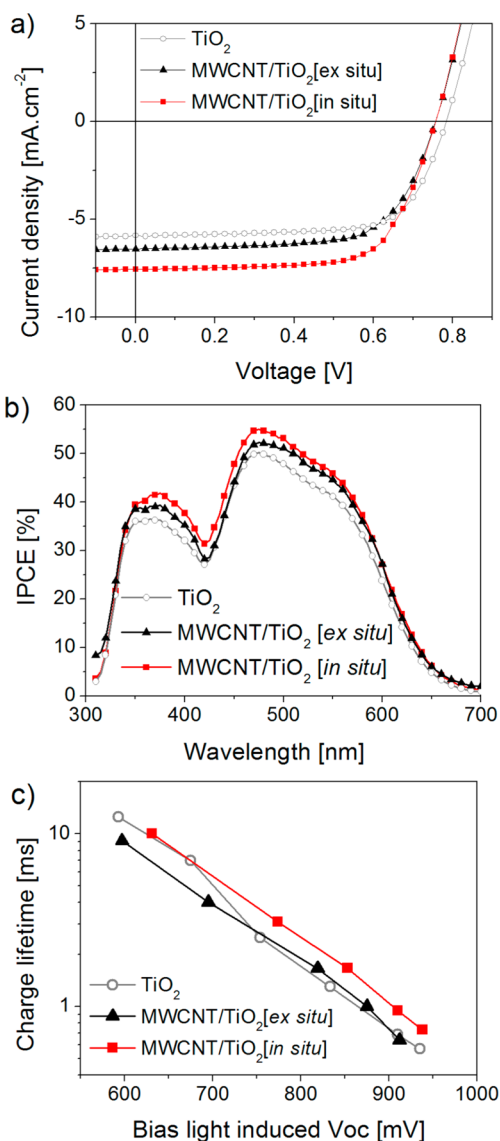
Figure 4. (a) Current density/voltage characteristics, (b) IPCE spectra, and (c) electron lifetimes extracted from transient photovoltage decay measurements for ssDSSC based on pure TiO_2 (open gray circles), MWCNT/TiO_2[ex situ] (solid black triangles), and MWCNT/TiO_2[in situ] (solid red squares) porous electrodes.

Table 1. Photovoltaic Parameters of ssDSSCs Based on the Pure TiO_2, ex Situ and in Situ TiO_2/MWCNTs Nanocomposites (100 mW cm^{-2}, AM1.5G)[a]

	V_{oc} (V)	J_{sc} (mA/cm^2)	FF (%)	η (%)
TiO_2	0.78	5.86	71	3.2
MWCNT/TiO_2[ex situ]	0.76	6.41	67	3.3
MWCNT/TiO_2[in situ]	0.75	7.57	69	3.9

[a]CNT content is 0.03 wt %.

The short-circuit current density (J_{sc}) clearly increases in the presence of MWCNTs in the porous electrode compared to the TiO_2 reference device, this increase being much more pronounced for the in situ (~29% increase) compared to the ex situ composite (~9%). This trend is confirmed by the incident photon to charge carrier efficiency (IPCE) spectra. Although all the cells show a comparable IPCE shape over the entire spectral range (300−600 nm), the in situ cell exhibits a

larger IPCE, indicating improved charge collection efficiency. Accordingly, the overall power conversion efficiency is significantly improved by about 20% by our in situ process. However, the open-circuit voltage of the cells slightly decreases in the presence of MWCNTs, as some shunts may occur, in accordance with related studies.[7,8] Further information on device operation can be obtained using transient photovoltage decay measurements, which is used to extract the effective electron lifetime for each cell under realistic working conditions (Figure 4c).

Compared to the pure and ex situ cells, a larger electron lifetime is evidenced using the in situ composite, especially for high bias induced open-circuit voltages, hence under high incident light intensities. The positive influence of CNTs on device performance can results from several effects. First, the better electronic interfacial interactions between the TiO_2 particles and the nanotubes induced by the in situ process can be accompanied by efficient charge injection from the metal oxide to MWCNT. This mechanism can efficiently improve the charge collection efficiency, leading to improved short-circuit current density and device overall performance. In this context, our analyses suggest that the in situ process can reduce the amount of interfacial trap states associated with the metal oxide particles compared to the mixed composite processed ex situ, as well as to the pure TiO_2 cell, and is therefore highly beneficial for charge lifetime and charge extraction. At the opposite, for the ex situ cell, the electron lifetime is found to be similar to that of the pure TiO_2 cell. This can arise from the low surface coverage of MWCNTs by TiO_2 particles observed in the porous layer (Figure 1d), which can cause some leakage of the photogenerated electrons to the electrolyte.[8] Moreover, poor TiO_2/MWCNTs electronic interactions, which result in a lower ability for TiO_2 surface passivation in the ex situ compared to the in situ case, are associated with intense interfacial recombination events. Such recombination is found to be further enhanced when the MWCNTs doping amount reaches 1 wt % in the ex situ composite (see Figure S10 in the Supporting Information), indicating that surface traps are also introduced by the MWCNTs when the grafted surface is weak. Therefore, the benefit of improved charge extraction is offset by the enhanced recombination in the ex situ case. In parallel, for a higher CNT content up to 0.09 wt %, the performance of the in situ device start to decrease (see Table S3 and Figure S11 in the Supporting Information), associated with a significant reduction in electron lifetime (see Figure S12 in the Supporting Information). This trend is likely to results from the occurrence of additional CNT/electrolyte interfaces at high nanotube contents, which favor detrimental electron back reactions. The direct optical absorption of the CNT can also screen the dye, leading to a reduced photocurrent for high nanotube loadings.[7]

Another beneficial effect that can be associated with the presence of CNT in the porous electrodes relates to the extraction of charges to the FTO electrode. Some studies devoted to carbon nanostructures associated with TiO_2 evidence the possibility to achieve stronger photocurrent because of a better charge extraction at this interface.[29] This effect, which can be observed below the percolation threshold, can also explain the improved charge lifetime in the devices. Further investigations are required in order to identify the relative contribution of this effect.

CONCLUSIONS

In summary, TiO_2/MWCNT nanocomposites were synthesized in situ and in a single step by laser pyrolysis. Compared to a direct postmixing of MWCNT with TiO_2, a dense coating of the nanotubes by metal oxide particles is evidenced, leading to enhanced electronic interactions between the two components. The nanotube dispersion in the TiO_2 powder is also found to be strongly improved by the in situ process. Efficient photoinduced electron transfers from the TiO_2 particles to MWCNTs are evidenced in this latter case using photoluminescence spectroscopy. Solid-state dye-sensitized solar cells based on in situ MWCNT/TiO_2 porous electrodes exhibit an enhanced efficiency associated with a larger short-circuit current density than that of cells based on ex situ postmixed MWCNT/TiO_2 composites. The intimate electronic interaction between the TiO_2 particles and MWCNTs is accompanied by a reduced charge recombination, resulting in an improved charge extraction to the electrode. This study demonstrates the relevance of laser pyrolysis for the synthesis and fine-tuning of the electronic properties of advanced composite materials, especially suitable for efficient photovoltaic energy conversion.

ASSOCIATED CONTENT

Ⓢ Supporting Information

Experimental details. FTIR and XRS spectra of MWCNTs. XRD patterns and TEM images of the nanopowders. Raman and PL spectra of in situ and ex situ composites. Photovoltaic performances and electron lifetime for ex situ ssDSSCs with different MWCNTs doping amounts. Current density−voltage characteristics and IPCE spectra of all analyzed devices. This material is available free of charge via the Internet at http://pubs.acs.org/.

AUTHOR INFORMATION

Corresponding Authors
*E-mail: johann.boucle@unilim.fr.
*E-mail: nathalie.herlin@cea.fr.

Notes
The authors declare no competing financial interest.

ACKNOWLEDGMENTS

REFERENCES

(1) Dang, X.; Yi, H.; Ham, M.-H.; Qi, J.; Yun, D. S.; Ladewski, R.; Strano, M. S.; Hammond, P. T.; Belcher, A. M. Virus-Templated Self-Assembled Single-Walled Carbon Nanotubes for Highly Efficient Electron Collection in Photovoltaic Devices. *Nat. Nanotechnol.* **2011**, *6*, 377−384.

(2) Chan, Y.; Wang, C.; Chen, B.-H.; Chen, C. Dye-Sensitized TiO_2 Solar Cells Based on Nanocomposite Photoanode Containing Plasma-Modified Multi-Walled Carbon Nanotubes. *Prog. Photovolt.: Res. Appl.* **2013**, *21*, 47−57.

(3) Liu, C.-T.; Wang, Y.-C.; Dong, R.-X.; Wang, C.-C.; Huang, K.-C.; Vittal, R.; Ho, K.-C.; Lin, J.-J. A Dual-Functional Pt/CNT TCO-free Counter Electrode for Dye-Sensitized Solar Cell. *J. Mater. Chem.* **2012**, *22*, 25311−25315.

(4) Benedetti, J. E.; Corrêa, A. a.; Carmello, M.; Almeida, L. C. P.; Gonçalves, A. S.; Nogueira, A. F. Cross-Linked Gel Polymer Electrolyte Containing Multi-Wall Carbon Nanotubes for Application in Dye-Sensitized Solar Cells. *J. Power Sources* **2012**, *208*, 263−270.

(5) Du, P.; Song, L.; Xiong, J.; Li, N.; Wang, L.; Xi, Z.; Wang, N.; Gao, L.; Zhu, H. Dye-Sensitized Solar Cells Based on Anatase TiO_2/Multi-Walled Carbon Nanotubes Composite Nanofibers Photoanode. *Electrochim. Acta* **2013**, *87*, 651−656.

(6) Guo, W.; Shen, Y.; Wu, L.; Gao, Y.; Ma, T. Performance of Dye-Sensitized Solar Cells Based on MWCNT/TiO_2-xNx Nanocomposite Electrodes. *Eur. J. Inorg. Chem.* **2011**, 1776−1783.

(7) Dembele, K. T.; Selopal, G. S.; Soldano, C.; Nechache, R.; Rimada, J. C.; Concina, I.; Sberveglieri, G.; Rosei, F.; Vomiero, A. Hybrid Carbon Nanotubes−TiO_2 Photoanodes for High Efficiency Dye-Sensitized Solar Cells. A. *J. Phys. Chem. C* **2013**, *117*, 14510−14517.

(8) Chen, J.; Li, B.; Zheng, J.; Zhao, J.; Zhu, Z. Role of Carbon Nanotubes in Dye-Sensitized TiO_2-Based Solar Cells. *J. Phys. Chem. C* **2012**, *116*, 14848−14856.

(9) Burschka, J.; Dualeh, A.; Kessler, F.; Baranoff, E.; Cevey-Ha, N.-L.; Yi, C.; Nazeeruddin, M. K.; Grätzel, M. Tris(2-(1H-pyrazol-1-yl)pyridine)cobalt(III) as p-type Dopant for Organic Semiconductors and its Application in Highly Efficient Solid-State Dye-Sensitized Solar Cells. *J. Am. Chem. Soc.* **2011**, *133*, 18042−18045.

(10) Service, R. F. Energy technology. Perovskite Solar Cells Keep on Surging. *Science* **2014**, *344*, 458−458.

(11) Golobostanfard, M. R.; Abdizadeh, H. Hierarchical Porous Titania/Carbon Nanotube Nanocomposite Photoanode Synthesized by Controlled Phase Separation for Dye Sensitized Solar Cell. *Sol. Energy Mater. Sol. Cells* **2014**, *120*, 295−302.

(12) Gui, M. M.; Chai, S.-P.; Xu, B.-Q.; Mohamed, A. R. Enhanced Visible Light Responsive MWCNT/TiO_2 Core−Shell Nanocomposites as the Potential Photocatalyst for Reduction of CO_2 into Methane. *Sol. Energy Mater. Sol. Cells* **2014**, *122*, 183−189.

(13) Vajda, K.; Mogyorosi, K.; Nemeth, Z.; Hernadi, K.; Forro, L.; Magrez, A.; Dombi, A. Photocatalytic Activity of TiO_2/SWCNT and TiO_2/MWCNT Nanocomposites with Different Carbon Nanotube Content. *Phys. Status Solidi B* **2011**, *248*, 2496−2499.

(14) Ou, Y.; Lin, J.; Fang, S.; Liao, D. MWNT−TiO_2:Ni Composite Catalyst: A New Class of Catalyst for Photocatalytic H_2 Evolution from Water under Visible Light Illumination. *Chem. Phys. Lett.* **2006**, *429*, 199−203.

(15) Muduli, S.; Lee, W.; Dhas, V.; Mujawar, S.; Dubey, M.; Vijayamohanan, K.; Han, S.-H.; Ogale, S. Enhanced Conversion Efficiency in Dye-Sensitized Solar Cells Based on Hydrothermally Synthesized TiO_2-MWCNT Nanocomposites. *ACS Appl. Mater. Interfaces* **2009**, *1*, 2030−2035.

(16) Yu, J.; Fan, J.; Cheng, B. Dye-Sensitized Solar Cells Based on Anatase TiO_2 Hollow Spheres/Carbon Nanotube Composite Films. *J. Power Sources* **2011**, *196*, 7891−7898.

(17) Swihart, M. Vapor Phase Synthesis of Nanoparticles. *Curr. Opin. Colloid Interface Sci.* **2003**, *8*, 127−133.

(18) Reau, A.; Guizard, B.; Mengeot, C.; Boulanger, L.; Tenegal, F. Large Scale Production of Nanoparticles by Laser Pyrolysis. *Mater. Sci. Forum.* **2007**, *534−536*, 85−88.

(19) Melhem, H.; Simon, P.; Beouch, L.; Goubard, F.; Boucharef, M.; Di Bin, C.; Leconte, Y.; Ratier, B.; Herlin-Boime, N.; Bouclé, J. TiO_2 Nanocrystals Synthesized by Laser Pyrolysis for the Up-Scaling of Efficient Solid-State Dye-Sensitized Solar Cells. *Adv. Energy Mater.* **2011**, *1*, 908−916.

(20) Simon, P.; Pignon, B.; Miao, B.; Coste-Leconte, S.; Leconte, Y.; Marguet, S.; Jegou, P.; Bouchet-Fabre, B.; Reynaud, C.; Herlin-Boime, N. N-Doped Titanium Monoxide Nanoparticles with TiO Rock-Salt

Structure, Low Energy Band Gap, and Visible Light Activity. *Chem. Mater.* **2010**, *22*, 3704−3711.

(21) Pignon, B.; Maskrot, H.; Guyot Ferreol, V.; Leconte, Y.; Coste, S.; Gervais, M.; Pouget, T.; Reynaud, C.; Tranchant, J.-F.; Herlin-Boime, N. Versatility of Laser Pyrolysis Applied to the Synthesis of TiO_2 Nanoparticles − Application to UV Attenuation. *Eur. J. Inorg. Chem.* **2008**, *2008*, 883−889.

(22) Castro, C.; Pinault, M.; Porterat, D.; Reynaud, C.; Mayne-L'Hermite, M. The Role of Hydrogen in the Aerosol-Assisted Chemical Vapor Deposition Process in Producing Thin and Densely Packed Vertically Aligned Carbon Nanotubes. *Carbon* **2013**, *61*, 585−594.

(23) Yu, J.-G.; Yu, H.-G.; Cheng, B.; Zhao, X.; Yu, J. C.; Ho, W. The Effect of Calcination Temperature on the Surface Microstructure and Photocatalytic Activity of TiO_2 Thin Films Prepared by Liquid Phase Deposition. *J. Phys. Chem. B* **2003**, *107*, 13871−13879.

(24) Rajasekar, K.; Thennarasu, S.; Rajesh, R.; Abirami, R.; Balkis Ameen, K.; Ramasubbu, A. Preparation of Mesoporous TiO_2/CNT Nanocomposites by Synthesis of Mesoporous Titania via EISA and their Photocatalytic Degradation under Visible Light Irradiation. *Solid State Sci.* **2013**, *26*, 45−52.

(25) Kernazhitsky, L.; Shymanovska, V.; Gavrilko, T.; Naumov, V.; Fedorenko, L.; Kshnyakin, V.; Baran, J. Room Temperature Photoluminescence of Anatase and Rutile TiO_2 Powders. *J. Lumin.* **2014**, *146*, 199−204.

(26) Melnyk, V.; Shymanovska, V.; Puchkovska, G.; Bezrodna, T.; Klishevich, G. Low-Temperature Luminescence of Different TiO_2 Modifications. *J. Mol. Struct.* **2005**, *744−747*, 573−576.

(27) Fujihara, K.; Izumi, S.; Ohno, T.; Matsumura, M. Time-Resolved Photoluminescence of Particulate TiO_2 Photocatalysts Suspended in Aqueous Solutions. *J. Photochem. Photobiol. A Chem.* **2000**, *132*, 99−104.

(28) Yu, Y.; Yu, J. C.; Chan, C.-Y.; Che, Y.-K.; Zhao, J.-C.; Ding, L.; Ge, W.-K.; Wong, P.-K. Enhancement of Adsorption and Photocatalytic Activity of TiO2 by Using Carbon Nanotubes for the Treatment of Azo Dye. *Appl. Catal. B* **2005**, *61*, 1−11.

(29) Dembele, K. T.; Selopal, G. S.; Milan, R.; Trudeau, C.; Benetti, D.; Soudi, A.; Natile, M. M.; Sberveglieri, G.; Cloutier, S.; Concina, I.; Rosei, F.; Vomiero, A. Graphene Below the Percolation Threshold in TiO_2 for Dye-Sensitized Solar Cells. *J. Mater. Chem. A* **2015**, DOI: 10.1039/C4TA04395B.